We are IntechOpen,
the world's leading publisher of
Open Access books
Built by scientists, for scientists

4,700
Open access books available

121,000
International authors and editors

135M
Downloads

Our authors are among the

154
Countries delivered to

TOP 1%
most cited scientists

12.2%
Contributors from top 500 universities

WEB OF SCIENCE™

Selection of our books indexed in the Book Citation Index
in Web of Science™ Core Collection (BKCI)

Interested in publishing with us?
Contact book.department@intechopen.com

Numbers displayed above are based on latest data collected.
For more information visit www.intechopen.com

Signal Processing in Holographic Data Storage

Tzi-Dar Chiueh and Chi-Yun Chen
National Taiwan University
Taipei, Taiwan

1. Introduction

Holographic data storage (HDS) is regarded as a potential candidate for next-generation optical data storage. It has features of extremely high capacity and ultra-fast data transfer rate. Holographic data storage abandons the conventional method which records information in one-dimensional bit streams along a spiral, but exploits two-dimensional (2-D) data format instead. Page access provides holographic data storage with much higher throughput by parallel processing on data streams. In addition, data are saved throughout the volume of the storage medium by applying a specific physical principle and this leads data capacity on the terabyte level.

Boosted data density, however, increases interferences between stored data pixels. Moreover, the physical limits of mechanical/electrical/optical components also result in misalignments in the retrieved images. Typical channel impairments in holographic data storage systems include misalignment, inter-pixel interferences and noises, which will be discussed in the following. One channel model that includes significant defects, such as misalignment, crosstalk among pixels, finite pixel fill factors, limited contrast ratio and noise, will also be introduced.

The overall signal processing for holographic data storage systems consists of three major parts: modulation codes, misalignment compensation, equalization and detection. A block diagram of such a system is illustrated in Fig. 1. Note that in addition to the three parts, error-correcting codes (ECC) help to keep the error rate of the retrieved information under an acceptable level. This topic is beyond the scope of the chapter and interested readers are referred to textbooks on error-correcting codes.

To help maintain signal fidelity of data pixels, modulation codes are designed to comply with some constraints. These constraints are designed based on the consideration of avoiding vulnerable patterns, facilitation of timing recovery, and simple decoder implementation. Modulation codes satisfying one or more constraints must also maintain a high enough code rate by using as few redundant pixels as possible. The details are discussed in the chapter on "Modulation Codes for Optical Data Storage."

Even with modulation codes, several defects, such as inter-pixel interferences and misalignments, can still cause degradation to the retrieved image and detection performance. Misalignments severely distort the retrieved image and thus are better handled before regular equalization and detection. Iterative cancellation by decision

feedback, oversampling with resampling, as well as interpolation with rate conversion are possible solutions for compensating misalignment.

Equalization and detection are the signal processing operations for final data decision in the holographic data storage reading procedure. Over the years, many approaches have been proposed for this purpose. For one, linear minimum mean squared error (LMMSE) equalization is a classical de-convolution method. Based on linear minimum mean squared error (LMMSE) equalization, nonlinear minimum mean squared error equalization can handle situations where there exists model mismatch. On the other hand, maximum likelihood page detection method can attain the best error performance theoretically. However, it suffers from huge computation complexity. Consequently, there have been several detection algorithms which are modifications of the maximum likelihood page detection method, such as parallel decision feedback equalization (PDFE) and two-dimensional maximum a posteriori (2D-MAP) detection.
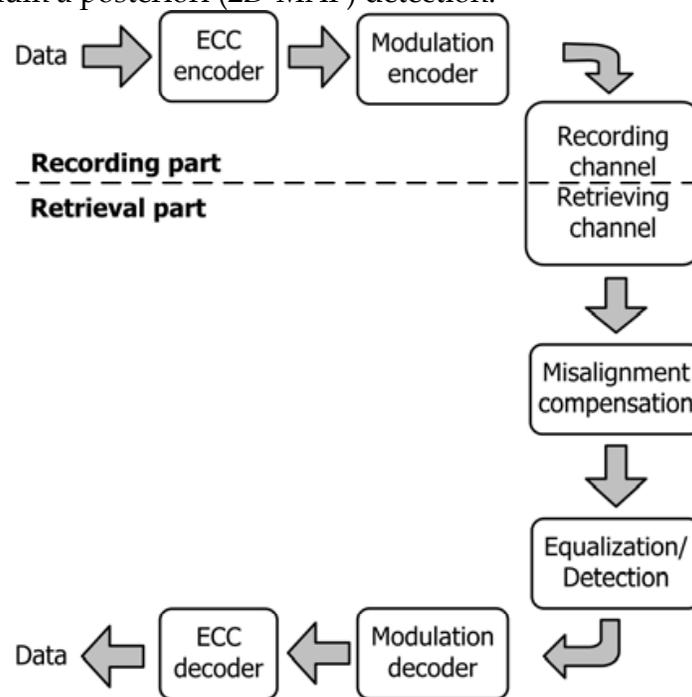

Fig. 1. Block diagram of signal processing in holographic data storage systems.

2. Recording and Retrieving Process

Holographic data storage systems store information carried by the interfered patterns within the recording media. The interfered pattern is created by one *object beam* and one *reference beam*. A *spatial light modulator* is adopted in holographic data storage systems to produce object beams, which is similar to a three-dimensional (3-D) object from which light is scattered and thus recorded in conventional holography. The spatial light modulator displays information in a 2-D format and modulates the intensity, phase or both intensity and phase of light beams. The 2-D data pages can consist of binary pixels (ON and OFF) or gray-scale pixels (Burr et al., 1998; Das et al., 2009). Spatial light modulators can be implemented by liquid crystal displays, digital micro-mirror devices, etc.
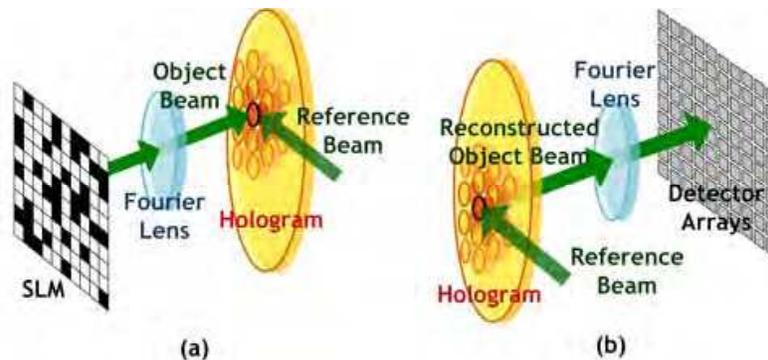
Fig. 2. Holographic data storage system: (a) recording process and (b) retrieving process (Chen et al., 2008).
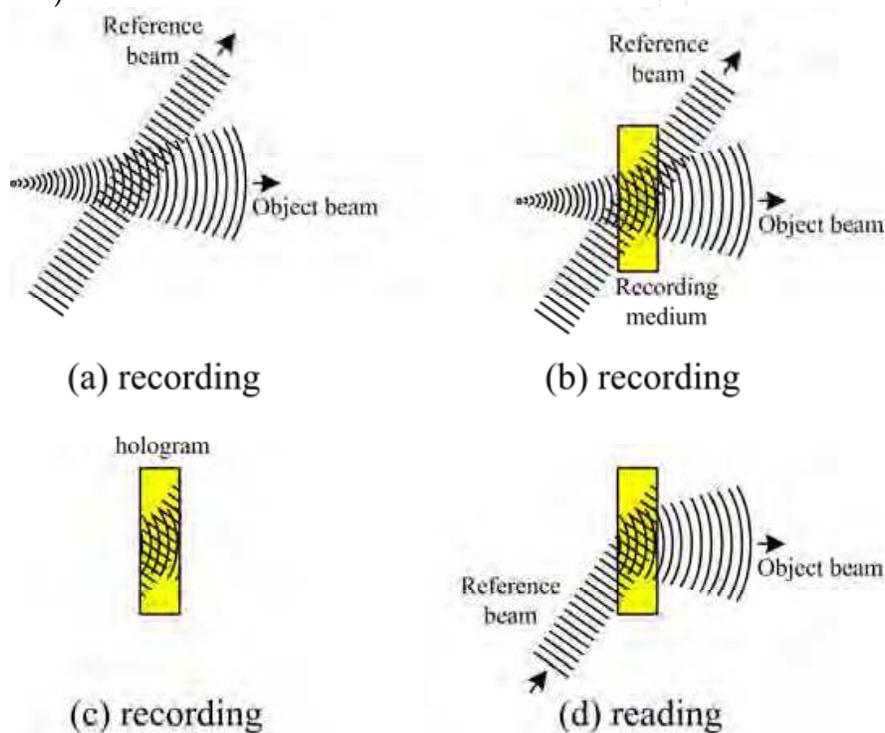

Fig. 3. Illustration of recording and reading process (InPhase).

With the spatial light modulator well controlled by the computer, information-carrying object beams can be created by passing a laser light through or being reflected by the spatial light modulator. Next, the object beam is interfered with a reference beam, producing an interferes pattern, namely, a *hologram*, which then leads to a chemical and/or physical change in the storage medium. By altering one or more characteristics of the reference beam, e.g., angle, wavelength, phase or more of them, multiple data pages can be superimposed at the same location. The process is called *multiplexing*. There are many multiplexing methods; interested readers can refer to (Coufal et al., 2000) for more details.

Reference beams of data pages at a certain location in the recording medium are like addresses of items in a table. In other words, data pages can be distinguished by the reference beam which interfered with the corresponding object beam. Therefore, by illuminating the recording medium with the reference beam from a proper incident angle, with a proper wavelength and phase, a certain object beam can be retrieved and then captured by the detector array at the receiving end. The stored information is processed by

transforming captured optical signals to electrical signals. The detector array is usually a charge coupled device (CCD) or a complementary metal oxide semiconductor (CMOS) image sensor. Minimum crosstalk from other pages when retrieving individual pages is attributed to a physical property called *Bragg effect*. Fig. 2 shows an example of the holographic data storage systems and Fig. 3 illustrates more details in the recording and reading processes.

3. Channel Defects

Ideally, a pixel of the spatial light modulator is directly imaged onto a detector pixel in a pixel-matched holographic data storage system. Such perfect correspondence is practically difficult to maintain due to non-ideal effects in holographic data storage channel that distort light signal and deteriorate signal fidelity. These non-ideal effects are called *channel defects*. Like most communication systems, optical storage systems have channel defects. Boosted storage density makes holographic data storage signals especially sensitive to interferences, noise or any tiny errors in storage media and optical/mechanical fabrication. From the spatial light modulator to the detector, from optical to mechanical, quite a few factors have significant influence on retrieved signals.

Laser light intensity determines the signal-to-noise ratio (SNR) but the intensity may not be uniform across the whole page. Usually, corners of data pages are darkerdue to the Gaussian wave front of the light source. This phenomenon and variations of light intensity over a page both are categorized as non-uniformity effect of light intensity. Non-uniformity of the retrieved signal level may cause burst errors at certain parts of data pages. Another factor is the contrast ratio, which is defined as the intensity ratio between an ON pixel and an OFF pixel. Ideally the contrast ratio is infinite. However, the OFF pixels actually have non-zero intensity in the spatial light modulator plane. A finite contrast ratio between the ON and OFF pixels makes the detection of pixel polarity more cumbersome. Another non-ideal effect is related to fill factors of spatial light modulator pixels and detector pixels. A fill factor is defined as the ratio of active area to the total pixel area, which is less than unity in real implementation.

Crosstalk is actually the most commonly discussed channel defect. We discuss two kinds of crosstalk here, including inter-pixel interference and inter-page interference. Inter-pixel interference is the crosstalk among pixels on the same data page. It results from any or combination of the following: band-limiting optical apertures, diffraction, defocus and other optical aberrations. Inter-page interference is caused by energy leakage from other data pages. This can be caused by inaccuracy of the reference beam when a certain data page is being retrieved. As more pages are stored in the medium, inter-page interference becomes a higher priority in holographic data storage retrieval. How good the interference can be handled determines to a large extent the number of date pages that can be superimposed.

Mechanical inaccuracies bring about another type of channel defects. Errors in the optical subsystem, mechanical vibration and media deformation can lead to severe misalignment, namely *magnification*, *translation* and *rotation*, between the recorded images and the retrieved images. Even without any inter-pixel interference or other optical distortions, misalignments still destroy the retrieval results entirely, especially in pixel-matched systems. Fig. 4 shows an example of misalignments $(\gamma_x, \gamma_y, \sigma_x, \sigma_y, \theta)$, where γ_x, γ_y are the magnification factors in the X- and Y- directions, respectively; σ_x, σ_y are the translation in the range of ±0.5 pixel

along the X- and Y- directions, respectively; and the rotation angle, θ, is positive in the counter-clockwise direction.
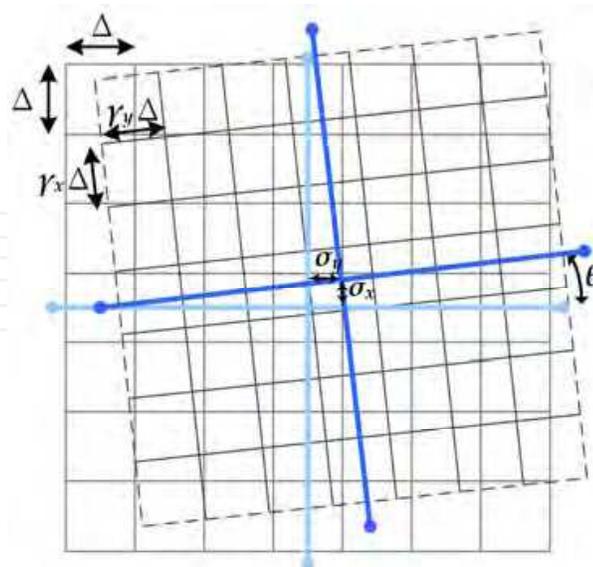

Fig. 4. Misalignment effects: magnification, translation and rotation of a detector page with respect to a spatial light modulator page.

Optical and electrical noises are inevitable in holographic data storage systems. They include crosstalk noise, scattering noise, shot noise and thermal noise. Optical noise occurs during the read-out process when the storage medium is illuminated by coherent reference beams, resulting from optical scatter, laser speckle, etc. Electrical noise, such as shot noise and thermal noise, occurs when optical signals are captured by detector arrays and converted into electrical signals.

4. Channel Model

A holographic data storage channel model proposed in (Chen et al., 2008), shown in Fig. 5, includes several key defects mentioned in Section 3. Multiple holographic data storage channel impairments including misalignment, inter-pixel interference, fill factors of spatial light modulator and CCD pixels, finite contrast ratio, oversampling ratio and noises are modeled. The input binary data sequence, $A(i, j)$, takes on values in the set $\{1, 1/\varepsilon\}$, where ε is a finite value called the amplitude contrast ratio. The spatial light modulator has a pixel shape function $p(x, y)$ given by

$$p(x,y) = \Pi\left(\frac{x}{ff_{SLM}\Delta}\right) \cdot \Pi\left(\frac{y}{ff_{SLM}\Delta}\right), \tag{1}$$

where ff_{SLM} represents the spatial light modulator's linear fill factor, the symbol Δ represents the pixel pitch and $\Pi(\cdot)$ is the unit rectangular function. Another factor that contributes to inter-pixel interference is the *point spread function*, a low-pass spatial behavior with impulse response $h_A(x, y)$ resulted from the limited aperture of the optics subsystem. This point spread function is expressed as

$$h_A(x, y) = h_A(x)h_A(y), \tag{2}$$

where

$$h_A(x) = (D/\lambda f_L)\text{sinc}(xD/\lambda f_L). \tag{3}$$

Note that D is the width of the square aperture, λ is the wavelength of the incident light, and f_L represents the focal length. The corresponding frequency-domain transfer function $H_A(f_x, f_y)$ in this case is the ideal 2-D rectangular low-pass filter with a cut-off frequency equal to $D/2\lambda f_L$.

A CCD/CMOS image sensor is inherently a square-law integration device that detects the intensity of the incident light. The image sensor transforms the incoming signals from the continuous spatial domain to the discrete spatial domain. Quantization in space causes several errors due to offsets in sampling frequency, location, and orientation. Magnification, translation and rotation are modeled as $(\gamma_x, \gamma_y, \sigma_x, \sigma_y, \theta)$, as explained previously. In addition, the oversampling ratio M, the pixel ratio between spatial light modulator and CCD/CMOS sensor, is another factor to be considered.

Taking all the aforementioned effects into account, we have the final image sensor output at the (k, l)th pixel position given by

$$C_m(k,l) = \int\int_{\Lambda_X \Lambda_Y}\left|\left[\sum_a\sum_b A(i+a,j+b)h(x-a\Delta,y-b\Delta)\right] + n_o(x',y')\right|^2 dy'dx' + n_e(k,l) \tag{4}$$

where

$$\Lambda_X = \left[\left(\frac{k-ff_{CCD}/2}{M\gamma_x}+\sigma_x\right)\Delta, \quad \left(\frac{k+ff_{CCD}/2}{M\gamma_x}+\sigma_x\right)\Delta\right]$$
$$\Lambda_Y = \left[\left(\frac{l-ff_{CCD}/2}{M\gamma_y}+\sigma_y\right)\Delta, \quad \left(\frac{l+ff_{CCD}/2}{M\gamma_y}+\sigma_y\right)\Delta\right] \tag{5}$$

and

$$x' = x\cos\theta + y\sin\theta$$
$$y' = -x\sin\theta + y\cos\theta \tag{6}$$

The subscript m in $C_m(k, l)$ indicates misalignment; $h(x, y)$ in Eq. (4) is also known as a *pixel spread function* and $h(x,y) = p(x,y) \otimes h_A(x,y)$; ff_{CCD} represents the CCD image sensor linear fill factor; $n_o(x', y')$ and $n_e(k, l)$ represent the optical noise and the electrical noise associated with the (k, l)th pixel, respectively. Translation and magnification effects are represented by varying the range of integration square as in Eq. (5), while the rotational effect is represented by transformation from the x-y coordinates to the x'-y' coordinates as in Eq. (6).

The probability density function of optical noise $n_o(x', y')$ can be described as a circular Gaussian distribution and its intensity distribution has Rician statistics. On the other hand, the electrical noise $n_e(k, l)$ is normally modeled as an additive white Gaussian noise with zero mean (Gu et al., 1996).
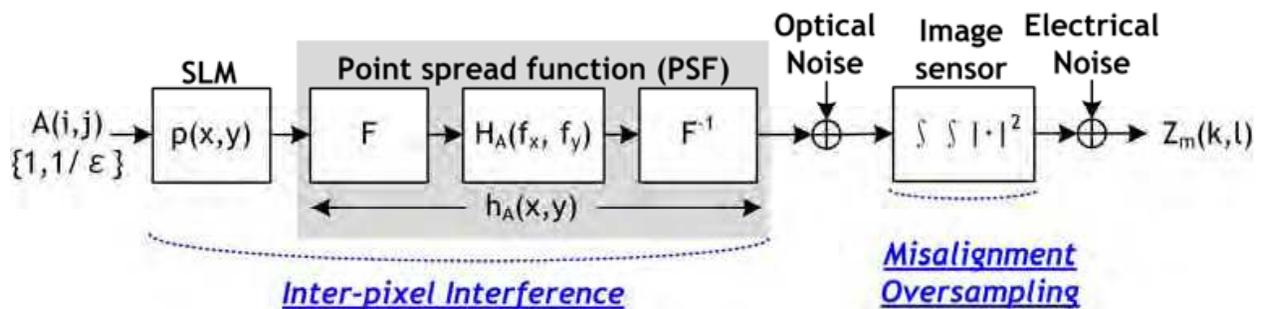
Fig. 5. Block diagram of a complete holographic data storage channel model.

5. Misalignment Compensation

Misalignments in retrieved images need be detected and compensated. To avoid information loss in the case that the detector array receives only part of a data page, a larger detector array or redundant (guard) pixels surrounding the information-carrying spatial light modulator pages can be employed. Moreover, a misalignment estimation procedure based on training pixels is needed before actual compensation. In fact, the estimation needs to be performed locally due to non-uniformity of channel effects. Toward this end, a page is divided into blocks of a proper size and training pixels are deployed in every block for local misalignment estimation. One possible estimation method is correlation based. In this method, the correlations of the received pixels and the known training pixels with different values of magnification, translation and rotation are first computed. The parameter setting with the maximum correlation is regarded as the estimation outcome. With the misalignments estimated, the retrieved images need be compensated before the modulation decoder decides the stored information. In the following several compensation schemes will be introduced.

5.1 Decision Feedback

Two decision feedback algorithms capable of dealing with translation and rotational misalignment compensation are proposed in (Menetrier & Burr, 2003) and (Srinivasa & McLaughlin, 2005), respectively. The iterative detection method exploits decision feedback to eliminate misalignment effects simultaneously. Hereafter, we explain the algorithm by using a one-dimensional translation effect in the pixel-matched system with a simplified channel model. A received pixel $C_m(k, l)$ can be represented as a function of two adjacent spatial light modulator pixels, $A(k-1, l)$ and $A(k, l)$, as shown in Fig. 6 and Eq. (7).
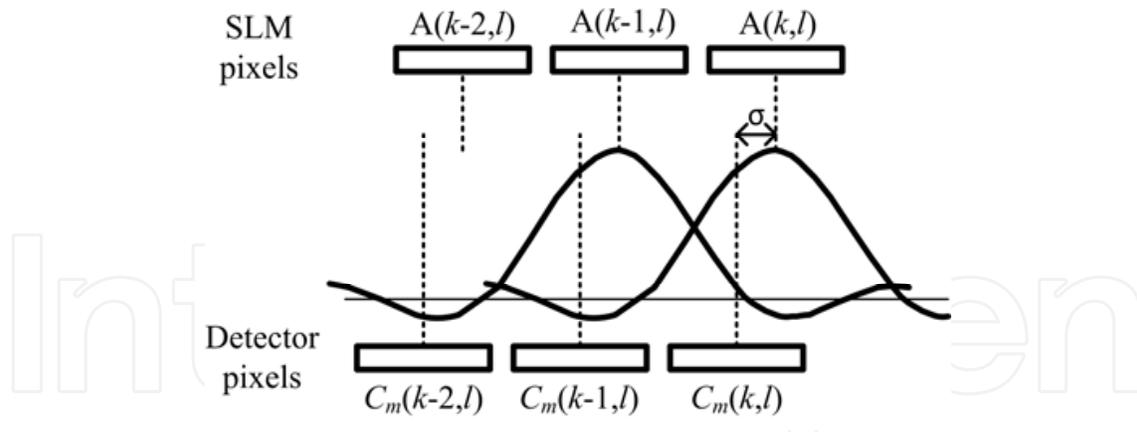
Fig. 6. Illustration of one-dimensional translation effect with parameter σ (Menetrier & Burr, 2003).

$$C_m(k,l) = \int_{-ff_{CCD}/2}^{ff_{CCD}/2} \int_{-ff_{CCD}/2}^{ff_{CCD}/2} \left[\sqrt{A(k,l)}h(x-\sigma,y) + \sqrt{A(k-1,l)}h(x-\sigma+1,y) \right]^2 dxdy \qquad (7)$$

Rewriting Eq. (7), we have

$$C_m(k,l) = A(k,l)H_{00}(\sigma) + 2\sqrt{A(k,l)A(k-1,l)}H_{01}(\sigma) + A(k-1,l)H_{11}(\sigma). \qquad (8)$$

It is clear that if $C_m(k, l)$ and $A(k-1, l)$ are known, $A(k, l)$ can be calculated according to Eq. (8). The decision feedback detection scheme is based on this observation. If σ is positive in the horizontal direction, then the scheme starts from the pixel at the top-left corner $C_m(0, 0)$, $A(0, 0)$ (the corner pixel) is first detected assuming that $A(-1, 0)$ is zero. With $A(0, 0)$ decided, decision feedback detection moves to detect the next pixel $A(1, 0)$ and repeats the same process until all pixels are detected. When the translation is only in the horizontal dimension, all rows can be processes simultaneously.

Extending the above case to 2-D, the retrieved pixel is a function of four spatial light modulator pixels

$$\begin{aligned} C_{m,s} = &A_s H_{ss} + A_h H_{hh} + A_v H_{vv} + A_d H_{dd} \\ &+ 2\sqrt{A_s A_h}H_{sh} + 2\sqrt{A_s A_v}H_{sv} + 2\sqrt{A_s A_d}H_{sd} \\ &+ 2\sqrt{A_h A_v}H_{hv} + 2\sqrt{A_h A_d}H_{hd} + 2\sqrt{A_v A_d}H_{vd} \end{aligned} \qquad (9)$$

where subscript s is for self, h for horizontal, v for vertical and d for diagonal. With the same principle used in the one-dimensional decision feedback detection, one must detect three pixels, horizontal, vertical and diagonal, before detecting the intended pixel. If both σ_x and σ_y are positive, again we start from the top-left pixel calculating $A(0, 0)$ assuming that pixel $A(0, -1)$, $A(-1, -1)$, and $A(-1, 0)$ are all zeros. The process is repeated row by row until all pixels are detected.

A similar detection scheme for images with rotational misalignment is proposed in (Srinivasa & McLaughlin, 2005). The process is somewhat more complicated because a pixel's relationship with associated SLM pixels depends on its location. For example, if the detector array has rotational misalignment of an angle in the clockwise direction as shown in Fig. 7, a pixel at the left top portion is a function of $A(k, l)$, $A(k, l-1)$, $A(k+1, l-1)$ and $A(k+1, l)$, while pixel at the right-bottom corner is a function of $A(k, l)$, $A(k-1, l)$, $A(k-1, l+1)$ and $A(k, l+1)$. Therefore, iterative decision feedback detection has to be performed differently

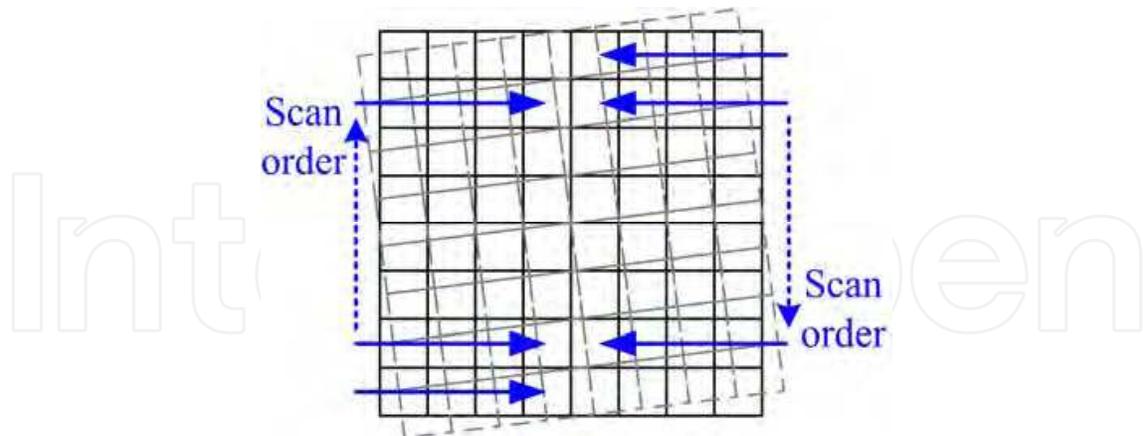depending on the location of the current pixel.

Fig. 7. Rotational misalignment entails different scan orders for the decision feedback cancellation detection in different portions of a page (Srinivasa & McLaughlin, 2005).

5.2 Oversampling and Resampling

Oversampling is a good way to handle the magnification effect and avoid the situation that a detector pixel is larger than a spatial light modulator pixel, leading to information loss. Besides, even if there is no magnification effect, a sub-Nyquist oversampling is necessary when the translation misalignment is around 0.5 pixel (Ayres et al., 2006b). With oversampling, the misalignment compensation task is no more than resampling.

The resampling process is actually a combination of misalignment compensation and equalization which will be discussed later. The resampling coefficients can be deduced by using the minimum mean-square-error (MMSE) criterion. With different sets of misalignment parameters, different sets of coefficients can be designed. For example, 20×20 sets of coefficients are required to handle 2-D translation misalignment with 5% precision. The number of coefficients needed to handle all possible misalignment situations can lead to a large memory size. Besides, oversampling uses more detector pixels to represent spatial light modulator pixels, thus decreasing stored information and recording density.

5.3 Interpolation and Rate Conversion

To compensate misalignments and convert the retrieved pixel rate to that of the stored data pixels, a 2-D filter capable of interpolation and rate conversion is proposed in (Chen et al., 2008). Interpolation can tackle translation and rotational misalignments. Rate conversion then converts the pixel rate to obtain pixel-matched pages free of misalignments.

Pixels in the captured images can be realigned by either 2-D interpolators or 2-D all-pass fractional delay filters (Pharris, 2005). A simple example is the bilinear filter shown in Fig. 8.
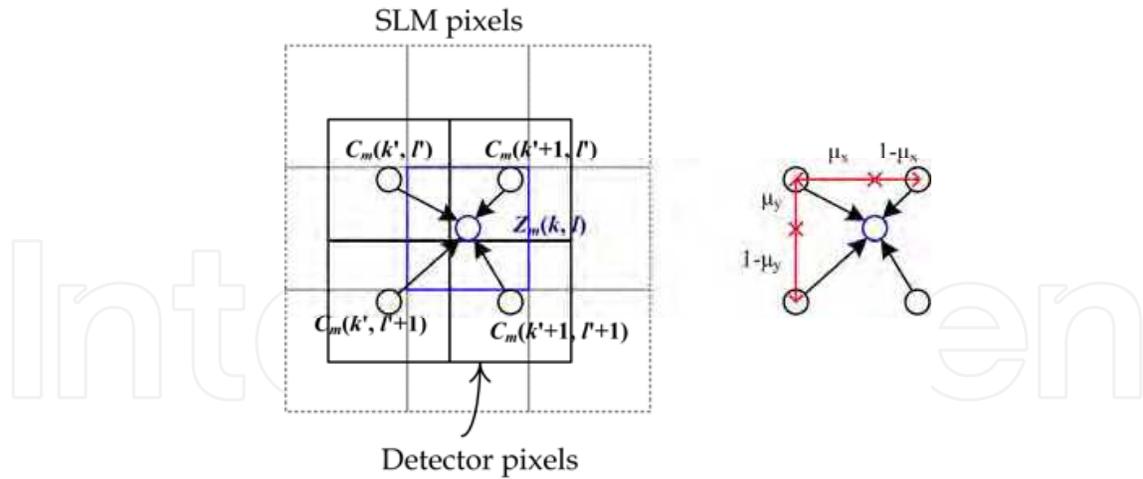
Fig. 8. Realignment by using a bilinear interpolator with local fractional displacement μ_x and μ_y.

The reconstructed pixel corresponding to a spatial light modulator pixel is given by

$$Z_m(k,l) = (1-\mu_x)\cdot(1-\mu_y)\cdot C_m(k',l') + \mu_x \cdot (1-\mu_y)\cdot C_m(k'+1,l')$$
$$+ (1-\mu_x)\cdot \mu_y \cdot C_m(k',l'+1) + \mu_x \cdot \mu_y \cdot C_m(k'+1,l'+1) \tag{10}$$

where Z_m and C_m are the realigned and misaligned images, respectively.
In general, the 2-D interpolator can be formulated as

$$Z_m(k,l) = \sum_{(p,q)\in S} f(\mu_x - p) f(\mu_y - q) C_m(k'+p,l'+q), \tag{11}$$

where $f(\cdot)$ is the one-dimensional impulse response of the corresponding interpolator; S is the input range of the 2-D interpolators; μ_x and μ_y indicate the local fractional displacement from the nearest pixel (k',l') at C_m in horizontal and vertical directions, respectively. The relationship between the local fractional displacement μ_x and μ_y and the corresponding pixel position k' and l' on the misaligned image C_m can be expressed as

$$\tilde{k} = (k\cos\theta - l\sin\theta + \sigma_x)\cdot M \cdot \gamma_x,$$
$$\tilde{l} = (k\sin\theta + l\cos\theta + \sigma_y)\cdot M \cdot \gamma_y \tag{12}$$

where M is the oversampling ratio and

$$k' = \lfloor \tilde{k} \rfloor, \quad \mu_x = \tilde{k} - k'$$
$$l' = \lfloor \tilde{l} \rfloor, \quad \mu_y = \tilde{l} - l' \tag{13}$$

To further enhance the realigned image quality, higher-order filters can be adopted. In (Chen et al., 2008), a 6×6-tap raised-cosine interpolator provides a better choice with acceptable complexity and satisfactory performance than other filters.
The rate-conversion filter can properly restore oversampled images that have suffered magnification effect to pixel-matched images for ensuing pixel detection. Without loss of generality, the rate-conversion filter can be formulated as

$$Z(i,j) = \sum_{p=P_{\min}}^{P_{\max}} \sum_{q=Q_{\min}}^{Q_{\max}} v_x(p) v_y(q) Z_m(k+p,l+q), \tag{14}$$

where Z_m indicates the realigned pixels and the weights $v_x(p)$ and $v_y(p)$ depend on the magnification factors γ_x and γ_y as well as the oversampling ratio M.

The realignment interpolator and the rate-conversion filter can be combined to reduce complexity. First, both 2-D filters are separated into two respective one-dimensional operations. Second, the realignment interpolators and the rate-conversion filters are integrated to construct a misalignment-compensation block that consists of one-dimensional compensation in the horizontal direction and one-dimensional compensation in the vertical direction. With such rearrangement, 84% reduction in additions and 74% reduction in multiplications are achieved (Chen et al., 2008).

6. Equalization and Detection

In general, equalization and detection is the final step of signal readout in holographic data storage. At this stage, most of the distortion caused by misalignments should have been removed. The remaining channel effects are mainly inter-pixel interference and noises. Equalization tries to eliminate impairments on the page by making its pixel intensity distribution as close to that of the spatial light modulator page as possible. A certain number of known pixels are needed to train the equalizer coefficients. For instance, assume that pixels on the distorted page are formulated as

$$\mathbf{Y} = \mathbf{HX+N}, \tag{15}$$

where $\mathbf{Y}$ indicates the pixels on the distorted page; $\mathbf{H}$ is the pixel spread function of the channel; $\mathbf{X}$ indicates the pixels on the SLM page and $\mathbf{N}$ indicates the noises. Equalization is done by computing $\mathbf{H}^{-1}\mathbf{Y}$, where $\mathbf{H}^{-1}$ denotes the equalizer coefficients. There are several well-known techniques for estimating these coefficients. However, as the holographic data storage channel is nonlinear, the simplistic linear equalizer may have model mismatch, making it ineffective.

Detection generates final decision for each pixel. The simplest detection is a slicer which determines a binary pixel as "1" if the intensity is higher than a certain threshold and "0" otherwise. The slicer must be preceded by equalization to achieve acceptable BER performance. There exist other detection algorithms that operate without equalization. However, they need additional channel state information for effective operation.

6.1 MMSE Equalization

LMMSE equalization is a popular equalization method in communication systems. In holographic data storage systems, LMMSE equalization has to be extended to two-dimensional (Singla & O'Sullivan, 2004; Chugg et al., 1999; Keskinoz & Vijaya Kumar, 1999; Choi & Baek, 2003; Ayres et al., 2006a). Assume that the 2-D equalizer has (2K-1)×(2K-1) taps and its output is given by

$$\hat{A}(i,j) = \sum_{m=-K}^{K} \sum_{n=-K}^{K} w(m,n)Z(i-m,j-n), \tag{16}$$

where $w(m, n)$ is the (m, n)th tap of the equalizer, and $Z(i, j)$ is the (i, j)th pixel of retrieved data page. The LMMSE equalizer calculates $w(m, n)$ that minimizes the average squared error between equalized output and actual stored pixel, i.e.,

$$\min\left\{ E\left[\left| \hat{A}(i,j) - A(i,j) \right|^2 \right] \right\}, \tag{17}$$

based on the MMSE criterion. According to the orthogonal principle (Haykin, 2002), we can make use of auto-correlation of the received pixels and the cross-correlation between the received and the desired pixels to solve for the optimal coefficients through the following equations

$$R_{AZ}(p,q) = \sum_{m=-K}^{K} \sum_{n=-K}^{K} w(m,n) R_{ZZ}(p-m, q-n) = w(p,q) \otimes R_{ZZ}(p,q), \qquad (18)$$

where $\otimes$ denotes convolution and

$$R_{AZ}(p,q) = E[A(i,j)Z(i-p, j-q)]$$
$$R_{ZZ}(p,q) = E[Z(i,j)Z(i-p, j-q)] \qquad (19)$$

(Keskinoz & Vijaya Kumar, 1999) provided a simple way to calculate equalizer coefficients by applying Fourier transformation to Eq. (18). The equalizer coefficients can then be obtained by

$$w(p,q) = IFFT\{FFT[R_{AZ}(p,q)] / FFT[R_{ZZ}(p,q)]\}. \qquad (20)$$

Unfortunately, linear equalizers can suffer from model mismatch and render them ineffective since the holographic data storage channel is inherently nonlinear. To this end, nonlinear equalization was also proposed (Nabavi & Vijaya Kumar, 2006; He & Mathew, 2006).

6.2 Parallel Decision Feedback Equalization

Decision feedback equalization was proposed in (King & Neifeld, 1998) and (Keskinoz & Vijaya Kumar, 2004). The algorithm iteratively detects pixels while considering the interferences from neighboring pixels based on decisions that have been made in the previous iterations. The process is executed on each pixel independently. The detection results will converge after several iterations. Hereafter in this chapter, we called this method *parallel decision feedback equalization (PDFE)*.

PDFE is actually a simplified version of the optimal maximum likelihood page detection algorithm which has a search space as large as an entire page and is thus impractical in actual implementation. PDFE breaks the whole page into small blocks whose size equals the extent of the channel pixel spread function and uses iterations to achieve near maximum likelihood performance.
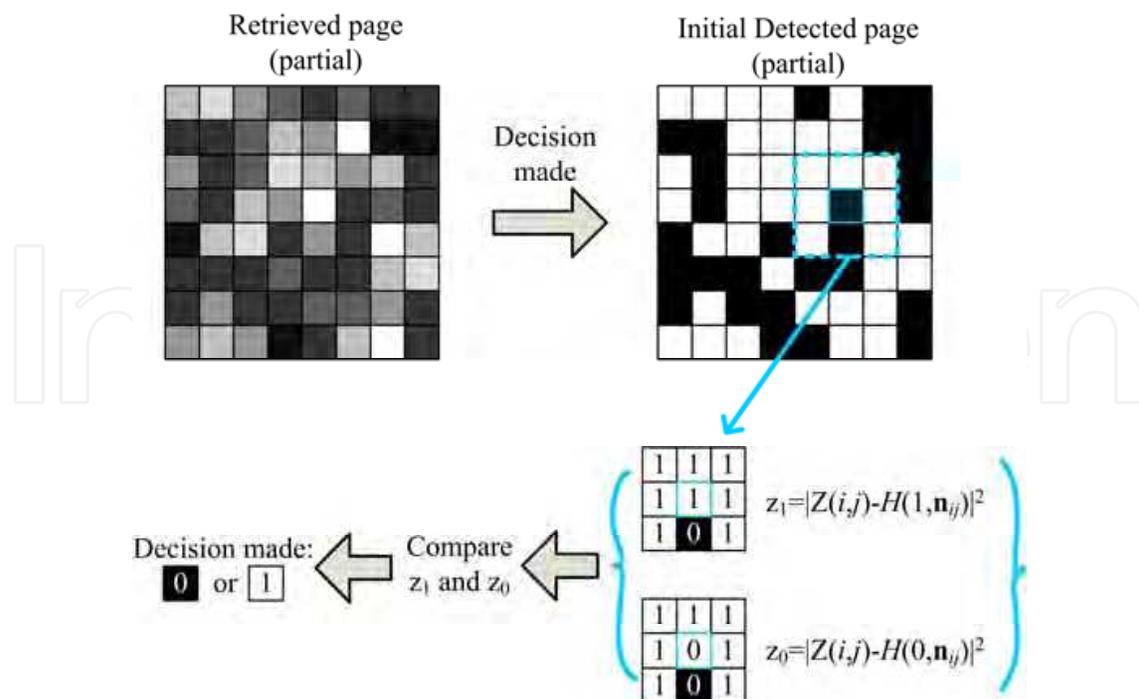
Fig. 9. Illustration of PDFE.

Assume that we consider inter-pixel interference within a range of 3×3 pixels and there exist no misalignment effects and the retrieved images have been made pixel-matched. Parallel decision feedback equalization starts with computing hard decision for each pixel. Then two hypotheses are tested to find the best decision for the current pixel. The process is shown in Fig. 9. With eight surrounding pixels given by decisions from the previous iteration, the central (current) pixel is decided as "1" or "0" according to

$$
\begin{aligned}
\hat{A}(i,j) = 1 \quad if \quad \left| Z(i,j) - H(1, \mathbf{n}_{ij}) \right|^2 < \left| Z(i,j) - H(0, \mathbf{n}_{ij}) \right|^2 , \\
\hat{A}(i,j) = 0 \quad if \quad \left| Z(i,j) - H(1, \mathbf{n}_{ij}) \right|^2 > \left| Z(i,j) - H(0, \mathbf{n}_{ij}) \right|^2
\end{aligned}
\tag{21}
$$

where $H(A(i,j), \mathbf{n}_{ij})$ is the inter-pixel-interference-inflicted channel output with $A(i,j)=0$ or 1 and a neighborhood pattern expressed as a binary vector, $\mathbf{n}_{ij}$, consisting of the eight binary pixels.

The performance of parallel decision feedback equalization depends on the correctness of channel estimation and good initial condition. With inaccurate channel information or too many errors in the initial condition, PDFE will have poor overall performance as initial errors can propagate throughout the entire page.

6.3 2D-MAP

Two-dimensional maximum a posteriori (2D-MAP) detection, proposed in (Chen et al., 1998) as the 2-D[4] (Two-Dimensional Distributed Data Detection) algorithm, is actually the well-known max-log-MAP algorithm. It is also a simplified sub-optimal maximum likelihood page detection algorithm. Different from PDFE, the extrinsic information of each pixel is now taken into consideration during searching for optimal decisions. Therefore, more than two cases are tested in 2D-MAP. In this algorithm, a log-likelihood ratio (LLR) for each pixel is used as extrinsic information and is maintained throughout the iterative process. An LLR

with higher absolute value indicates a greater probability of the pixel being "1" or "0." As the iteration goes on, the LLR value at each pixel will be re-calculated based on the knowledge of the previous LLR values of its eight neighbors. In all likelihood, this process makes each and every LLR move away from the origin and all pixel decisions become more and more certain.

The procedure of the 2D-MAP detection comprises *likelihood computation* and *update*. In a binary holographic data storage system, the likelihood computation formulas are given by

$$LL1_U^{(k)}(i,j) = \min_{N_{ij}} \left\{ \frac{1}{2N_0} \left| Z(i,j) - H(1,\mathbf{n}_{ij}) \right|^2 + \mathbf{d}_{ij}^{(k-1)} \bullet \mathbf{n}_{ij} \right\}.$$
$$LL0_U^{(k)}(i,j) = \min_{N_{ij}} \left\{ \frac{1}{2N_0} \left| Z(i,j) - H(0,\mathbf{n}_{ij}) \right|^2 + \mathbf{d}_{ij}^{(k-1)} \bullet \mathbf{n}_{ij} \right\}$$

(22)

Again $H(A(i,j), \mathbf{n}_{ij})$ is the inter-pixel interference-inflicted channel output with $A(i,j) = 0$ or 1 and a neighborhood pattern expressed as a binary vector, $\mathbf{n}_{ij}$, consisting of the eight binary pixels; N_{ij} is the set of all possible neighborhood patterns. In addition, $\mathbf{d}^{(k-1)}$ is a vector consisting of the corresponding LLR values of neighboring pixels in the $(k-1)^{th}$ iteration and the symbol '$\bullet$' represents inner product of two vectors. In the above, all misalignment effects and oversampling have been properly handled and the only remaining channel effect is inter-pixel interference and noises. LLRs are updated at the end of each iteration. To avoid sudden changes in the LLR values, a forgetting factor β is applied and the updated LLR takes the form of

$$L^{(k)}(i,j) = (1-\beta)L^{(k-1)}(i,j) + \beta \left\{ LL1_U^{(k)}(i,j) - LL0_U^{(k)}(i,j) \right\},$$

(23)

The value of β can affect the speed and accuracy of convergence. A larger β leads to faster convergence but may lead to poor detection performance.

With the help of soft information, 2D-MAP indeed has better performance but with much higher complexity than PDFE. In (Chen et al., 2008) several complexity reduction schemes, including iteration, candidate, neighborhood and addition reduction, are proposed and thus up to 95% complexity is saved without compromising the detection performance.

7. Conclusion

This chapter gives an overview to the processing of retrieved signals in holographic data storage systems. The information to be stored is arranged in a 2-D format as binary or gray-level pixels and recorded by interference patterns called hologram. The fact that multiple holograms can be superimposed at the same location of the recording medium leads to volume storage that provides very high storage capacity.

Two important channel defects, misalignments and inter-pixel interferences, are major causes for degradation in detection performance and their model is formulated mathematically. Several misalignments compensation algorithms are introduced. One algorithm adopts decision feedback to handle misalignments and interference simultaneously. Pixels are detected one by one after cancelling interference from neighboring pixels. The scan orders should be carefully designed when misalignments may involve pixels coming from other directions. Another algorithm makes use of oversampling, and then resample at location. Another algorithm combines interpolation and rate conversion to compensate various misalignments effects.

Equalization and detection are crucial steps in restoring stored information from the interference-inflicted signal. Albeit its popularity and low complexity, LMMSE equalization algorithm suffers from the problem of model mismatch as the holographic data storage channel is inherently nonlinear. In light of this fact, two nonlinear detection algorithms, both simplified versions of the optimal maximum likelihood page detection, are introduced. They achieve better performance than the LMMSE method at the cost of higher complexity.

8. References

Ayres, M.; Hoskins, A., & Curtis, K. (2006a). Processing data pixels in a holographic data storage system. WIPO patent (Sep. 2006) WO/2006/093945 A2

Ayres, M.; Hoskins, A., & Curtis, K. (2006b). Image oversampling for page-oriented optical data storage. *Applied Optics*, Vol. 45, No. 11, pp. 2459–2464, ISSN 0003-6935

Burr, G. W.; Coufal, H., Hoffnagle, J. A., Jefferson, C. M., & Neifeld, M. A. (1998). Gray-scale data pages for digital holographic data storage. *Optics Letters*, Vol. 23, No. 15, pp. 1218–1220, ISSN 0146-9592

Chen, X.; Chugg, K. M. & Neifeld, M. A. (1998). Near-optimal parallel distributed data detection for page-oriented optical memories. *IEEE J. Sel. Top. Quantum Electron.*, Vol. 4, No. 5, pp. 866–879, ISSN 1077-260X

Chen, C.-Y.; Fu, C.-C. & Chiueh, T.-D. (2008). Low-complexity pixel detection for images with misalignments and inter-pixel interference in holographic data storage. *Applied Optics*, vol. 47, no. 36, pp. 6784–6795, ISSN 0003-6935

Choi, A.-S. & Baek, W.-S. (2003). Minimum mean-square error and blind equalization for digital holographic data storage with intersymbol interference. *Jpn. J. Appl. Phys.*, Vol. 42, No. 10, pp. 6424–6427, ISSN 0021-4922

Chugg, K. M.; Chen, X., Neifeld, M. A. (1999). Two-dimensional equalization in coherent and incoherent page-oriented optical memory. *J. Opt. Soc. Am. A*, Vol. 16, No. 3, pp. 549–562, ISSN 1084-7529

Coufal, H. J.; Psaltis, D. & Sincerbox, G. T. (Eds.). (2000). *Holographic data storage,* Springer-Verlag, ISBN 3-540-66691-5, New York

Das, B.; Joseph, J., Singh, K. (2009). Phase modulated gray-scale data pages for digital holographic data storage. *Optics Communications*, Vol. 282, No. 11, pp. 2147–2154, ISSN 0030-4018

Gu, C.; Dai, F., & Hong, J. (1996). Statistics of both optical and electrical noise in digital volume holographic data storage. *Electronic Letters,* Vol. 32, No. 15, pp.1400–1402, ISSN 0013-5194

Haykin, S. (2002). *Adaptive filter theory*, Prentice Hall, 4th edition, ISBN 0130901261

He, A. & Mathew, G. (2006). Nonlinear equalization for holographic data storage systems. *Applied Optics*, Vol. 45, No. 12, pp. 2731–2741, ISSN 0003-6935

InPhase website: http://www.inphase-technologies.com

Keskinoz, M. & Vijaya Kumar, B. V. K. (1999). Application of linear minimum mean-squared-error equalization for volume holographic data storage. *Applied Optics*, Vol. 38, No. 20, pp. 4387–4393, ISSN 0003-6935

Keskinoz M. & Vijaya Kumar, B. V. K. (2004). Discrete magnitude-squared channel modeling, equalization, and detection for volume holographic storage channels. *Applied Optics*, Vol. 43, No. 6, pp. 1368–1378, ISSN 0003-6935

King, B. M. & Neifeld, M. A. (1998). Parallel detection algorithm for page-oriented optical memories. *Applied Optics*, Vol. 37, No. 26, pp. 6275–6298, ISSN 0003-6935

Menetrier, L. & Burr, G. W. (2003). Density implications of shift compensation postprocessing in holographic storage systems. *Applied Optics*, Vol. 42, No. 5, pp. 845–860, ISSN 0003-6935

Nabavi, S. & Vijaya Kumar, B. V. K. (2006). Application of linear and nonlinear equalization methods for holographic data storage. *Jpn. J. Appl. Phys.*, Vol. 45, No. 2B, pp. 1079–1083, ISSN 0021-4922

Pharris, K. J. (2005). Methods and systems for holographic data recovery. *U.S. Patent* (Jan. 2005) 20050018263 A1

Singla, N. & O'Sullivan, J. A. (2004). Minimum mean squared error equalization using priors for two-dimensional intersymbol interference. *Proceedings of IEEE International Symposium on Information Theory (ISIT)*, pp. 130, ISBN 0-7803-8280-3, Jun. 2004, Chicago

Srinivasa, S. G. & McLaughlin, S. W. (2005). Signal recovery due to rotational pixel misalignments. *Proceedings of IEEE International Conference on Acoustics, Speech, and Signal Processing (ICASSP)*, Vol. 4, iv/121- iv/124, ISBN 0-7803-8874-7, Mar. 2005, Philadelphia

Data Storage

Edited by Florin Balasa

ISBN 978-953-307-063-6

Hard cover, 226 pages

Publisher InTech

Published online 01, April, 2010

Published in print edition April, 2010

The book presents several advances in different research areas related to data storage, from the design of a hierarchical memory subsystem in embedded signal processing systems for data-intensive applications, through data representation in flash memories, data recording and retrieval in conventional optical data storage systems and the more recent holographic systems, to applications in medicine requiring massive image databases.

How to reference

In order to correctly reference this scholarly work, feel free to copy and paste the following:

Tzi-Dar Chiueh and Chi-Yun Chen (2010). Signal Processing in Holographic Data Storage, Data Storage, Florin Balasa (Ed.), ISBN: 978-953-307-063-6, InTech, Available from: http://www.intechopen.com/books/data-storage/signal-processing-in-holographic-data-storage

INTECH
open science | open minds